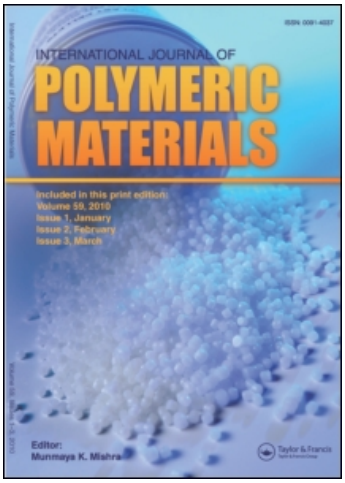

International Journal of Polymeric Materials
Publication details, including instructions for authors and subscription information:
http://www.informaworld.com/smpp/title~content=t713647664

Manufacturing, Morphology and Mechanical Properties of Carbon and Glass Fiber-Polyamide 12 Composite Laminates

M. Evstatiev[a]; K. Friedrich[b]; S. Fakirov[a]
[a] Laboratory on Structure and Properties of Polymers, Sofia University, Sofia, Bulgaria [b] Institute for Composite Materials (Ltd.), University of Kaiserslautern, Kaiserslautern, Germany

To cite this Article Evstatiev, M. , Friedrich, K. and Fakirov, S.(1993) 'Manufacturing, Morphology and Mechanical Properties of Carbon and Glass Fiber-Polyamide 12 Composite Laminates', International Journal of Polymeric Materials, 19: 1, 29 — 40
To link to this Article: DOI: 10.1080/00914039308012015
URL: http://dx.doi.org/10.1080/00914039308012015

Intern. J. Polymeric Mater., 1993, Vol. 19, pp. 29–40
Reprints available directly from the publisher
Photocopying permitted by license only

Printed in Malaysia

Manufacturing, Morphology and Mechanical Properties of Carbon and Glass Fiber-Polyamide 12 Composite Laminates

M. EVSTATIEV,† K. FRIEDRICH‡ and S. FAKIROV†

†Laboratory on Structure and Properties of Polymers, Sofia University, 1126 Sofia, Bulgaria;
‡Institute for Composite Materials (Ltd.), University of Kaiserslautern, 6750 Kaiserslautern, Germany

(Received April 22, 1992)

In this paper the influence of thermal pre-history of continuous carbon and glass fiber reinforced polyamide 12 composites on the morphology of the polymer matrix is studied. Of further interest is the effect of the later on the mechanical properties of the laminates.

WAXS, DSC, hot-stage light microscopy and density measurements are used to determine the structure and crystallization rate of the samples. It is established that carbon fiber-containing laminates show a faster crystallization rate, a relatively high crystallinity and high values of the flexural strength and modulus. However, these samples show lower energies of delamination as revealed by mode I and mode II tests when compared to the corresponding glass fiber-reinforced composites.

KEY WORDS Morphology, carbon fiber, polyamide, composites, interlaminar fracture toughness.

I. INTRODUCTION

It has been admitted that toughness in general, and interlaminar fracture toughness more specifically is a major critical composite property for structures subjected to impact loading during technical service. Different solutions have been proposed to improve the interlaminar toughness, and hence the delamination resistance. One of these solutions is the use of a tougher polymer as matrix material.

The new generation of thermoplastic matrix composites offers some more advantages among which are the longer storage life of the intermediate material forms, repeatable forming, weldability, recyclability, better damage tolerance and higher interlaminar fracture toughness. On the other hand, impregnation of the fibers with the rather viscous thermoplastic melt, in such a way that the fibers are well wetted all over, is more difficult than for uncured thermosets. Although this can be overcome by impregnation with thermoplastics in solution, this technique is rather difficult, time consuming and combined with health risks if not done properly. Therefore, composite intermediate material suppliers developed different new methods: film stacking, co- or intermingled polymer and carbon or glass fibers, pultruded tapes, and polymer powder impregnated fiber bundles.

In this study the powder impregnated fiber bundles as an intermediate material form were used to process unidirectional fiber reinforced specimens. Considering reinforced thermosets, the assumption is usually made, that the polymer matrix remains basically unaffected by the introduction of the reinforcing phase. Because of the different effects of fibers on the crystallization of semi-crystalline thermoplastics during processing, this assumption is expected to be not valid any more. In addition crystallization is affected by the thermal prehistory after consolidation of the material. It was attempted here to evaluate the influences of the type of the reinforcing component and the thermal pre-history (in particular cooling rate) of continuous carbon (CF) and glass fiber (GF) reinforced polyamide 12 (CF-, GF-PA 12) composites on the structure of the polymer matrix as well as the influence of this structure on the mechanical properties of the laminates. In a preliminary study of the authors[1] this influence of thermal treatment on the interlaminar fracture behaviors of GF-PA 12 composites was followed.

II. EXPERIMENTAL

II.1. Material and Manufacturing of the Samples

The material investigated is a commercial product of ENICHEM (Italy), i.e. FIT® (fibre impregnated thermoplastics) consisting of:

—a continuous bundle of 6,000 individual carbon (Torayca 6 K, 68 w/o) or E-glass fibers (Fiberglass 2400 Tex, 70 w/o),

—PA 12 powder between them (particular diameter similar to that of the fibers),

—a PA 12 sheath around the whole bundle.[2]

The single bundles were designated as GF-FIT and CF-FIT in that what follows.

Consolidation of these intermediate material forms into prepregs (preimpregnated sheets) was carried out in a heat press using a steel mold. Each resulting prepreg contained 7 (for GF-FIT) or 10 (for CF-FIT) parallel fiber bundles. In a second step 8 (for GF) or 12 (for CF) of these one-layer prepregs were stacked into the mold to obtain either $[0]_8$ or $[0]_{12}$ unidirectional reinforced laminates. The processing conditions were optimized as follows: After heating up the system above the melting temperature of PA 12 (T_m = 180°C), i.e. up to 220°C at a pressure of 1 MPa for 3 min, a compressive load of 15 kN (i.e. a pressure of 6 MPa) was applied over a period 5 min. Then a fast cooling rate of 250°C/min (samples A (CF) and D (GF)) or a slow cooling rate of 10°C/min (samples B (CF) and E (GF)) were used in order to achieve low and high crystallinity, respectively. In addition, laminates of type B and E were then annealed for 3 hrs at 150°C in order to further increase the crystallinity (samples C (CF) and F (GF)).

During manufacturing of the laminates, a double layer capton foil was placed between the 4th and 5th (for GF laminates) or between the 6th and 7th (for CF laminates) layers at one end of the specimens in order to define starter cracks for interlaminar fracture toughness tests.

II.2. Structural Characterizations

In order to characterize the morphology of the different specimen types (A, B, C CF-containing and D, E, F GF-containing laminates), DSC, WAXS, hot-stage polarized microscopy and density measurements were performed.

The DSC measurements were carried out using a Mettler TA 3000 apparatus at a scanning rate of 10°C/min during heating and cooling and a sample mass of about 20 mg (including the fibers). From the melting and crystallization peaks the apparent degrees of crystallinity w_c (DSC) and x_c (DSC), respectively were determined after isothermal (T = 160°C) and non-isothermal crystallization from the melt. Use was made of the formulas w_c (DSC) = $\Delta H_m/\Delta H°$ and x_c (DSC) = $\Delta H_c/\Delta H°$, where ΔH_m is the heat of fusion and ΔH_c is the heat of crystallization; the reference value for PA 12 amounted to $\Delta H°$ = 134 kJ/kg.[3]

From the S-shaped curves of isothermal crystallization at 160°C, the rate constant (K), the Avrami constant (n), the induction period (τ) and the crystallization half time ($\tau_{1/2}$) of pure PA 12 and CF- and GF-containing laminates were calculated.

Wide angle X-ray scattering (WAXS) measurements were performed on a D 500 Siemens diffractometer using Ni-filtered CuKα radiation. The size of the crystallites was estimated from the transmission meridional diffractograms of the samples using the Scherrer formula.[4] In addition WAXS transmission photographs were taken.

The observation of the crystalline structure in the bulk polymer and in the vicinity of the fibers was performed under polarized light with a Zeiss Opton light microscope equipped with a Mettler heating stage and a photographic set. By means of a recording unit, the S-shaped curves of isothermal and non-isothermal crystallization were obtained.

The samples' densities were determined by means of a gradient column containing a carbon tetrachloride/*n*-heptane mixture for both sample types.

II.3. Mechanical Tests

II.3.1. Flexural response. These studies were performed on a Zwick 1464 dynamometer equipped with a standard device for three-point bending (3 PB) tests at a cross-head speed of 1 mm/min. The strength (σ_{max}) and modulus (E_{flex}) were calculated from the stress/strain curves using the following formulas[5]: $\sigma_{max} = 3F_{max} L/2wh^2$ and $E_{flex} = FL^3/4wh^3\delta$, where F is the force, δ the deflection and L the sample length.

The GF-PA 12 laminates were 4–4.3 mm thick (h) with an L/h ratio of about 25, while these values were 2.6–3 mm and about 34, respectively in the case of CF-PA 12 laminates. The width of the specimens (w) amounted to about 20 mm in all cases.

II.3.2. Double cantilever beam (DCB) test (mode I). DCB test were performed with CF-PA 12 laminates only since the GF-PA 12 samples were already studied in a previous investigation.[1] Loading was introduced via bonded hinges, through which the specimen could be opened continuously at room temperature and a cross-head speed of 1 mm/min. The starting crack length of the samples were 40–45 mm. Application of the simple beam theory method lead to the determination of

the critical strain energy release rate via $G_{Ic} = 3F_c\delta/2wa$, where "a" is the crack length and F_c the critical load at crack instability.[5]

II.3.3. End notched flexure (ENF) test (mode II). This method covers the determination of the critical strain energy release rate (G_{IIc}) for delamination crack propagation under in-plane shear loading. The specimen is loaded in a three-point bending fixture at a cross-head speed of 0.5 mm/min at room temperature. The method for determining G_{IIc} follows again the simple beam theory[5]: $G_{IIc} = 9a^2F_c\delta/2w(2L^3 + 3a^3)$.

III. RESULTS AND DISCUSSION

III.1. Structure of the Polymer Matrix

Polyamide 12 (PA 12) is a semi-crystalline polymer; its crystalline phase is mainly built up within a spherulitic super-structure. Photographs of isothermally (a) and non-isothermally (b) crystallized PA 12 melts containing a small amount of carbon fibers are shown in Figure 1. A random distribution of the spherulites in the bulk sample is observed, their size ranging from 10 to 80 μm. However, a substantial difference in the number, size and shape of the spherulites created by different types of crystallization is not visible.

Two types of reflections differing in their shapes and origin are observed in the WAXS patterns presented in Figure 2 (CF-PA 12, sample B, Figure 2a, and GF-PA 12, sample E, Figure 2b).

Two concentric circles—the stronger one located at 2θ of about 20° belong to the first type. These reflections originating from the polymer matrix indicate its isotropic state and the random distribution of crystallites in the bulk of the sample. The second type of reflections (Figure 2a) is concentrated in the equatorial direction, being placed at wider scattering angles (2θ of about 25°) and is due to the carbon fibers. It suggests an orientation and alignment of the reinforcing elements along the sample axis as well as a rather perfect orientation of the fibers themselves. This type of reflections is absent in the case of glass fiber reinforced materials (Figure 2b).

Transmission WAXS diffractograms in the meridional (a) and equatorial (b) direction of pure PA 12, CF-FIT, CF and CF-containing PA 12 of types A, B and C are presented in Figure 3. From the shape of the sample A curve, it can be concluded that, although rapidly cooled, this sample contains a substantial amount of crystallites. The sharpening of the reflections at $2\theta \sim 20°$ in case of the slowly cooled sample B and the additionally annealed sample C, indicates some increase of the perfection of the crystallites. The data on the crystallite size (D) in samples A, B and C shown in Table I suggest that this structural parameter is almost independent of the thermal pre-history. However, the latter affects slightly the sample density (ρ) which increases in the order from A to C (Table I) due to increased amount and perfection of the crystallites as it can be concluded from the scattering curves (Figure 3). Concerning the GF-containing laminates (samples D, E and F), it can be noted that the same increase of the crystallite size takes place together with the density rise (from D to F, Table I).

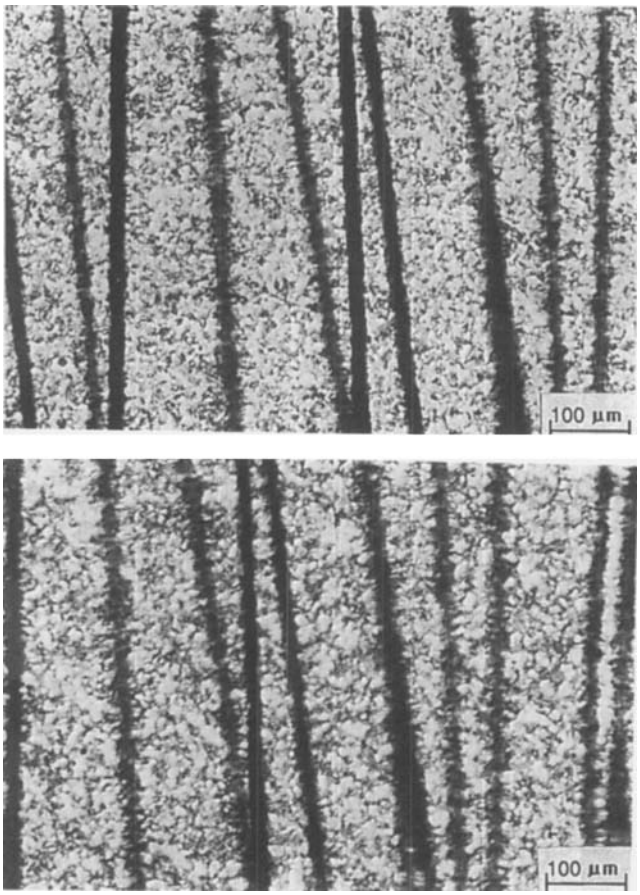

FIGURE 1 Polarized light microscopy photographs of PA 12 containing a small number of carbon fibers and crystallized from the melt under isothermal (a) and non-isothermal (b) conditions. The pictures are taken at the same place after repeating melting.

Data on the degree of crystallinity calculated from the DSC curves of melting (w_c (DSC)) of all samples studied are presented in Table I as well. It can be seen that the difference in w_c of samples B and C as well as that of samples E and F are insignificant, indicating that the different thermal pre-history (slow cooling and additional annealing) does not affect substantially the degree of crystallinity of the polymer in these laminates. Strikingly enough, however, the highest w_c values are obtained for the rapidly cooled samples A and D (Table I). It should be noted that these values are unrealistic and due to additional crystallization prior to melting at 180°C, as proved by the exothermal peak observed at about 160°C. The high w_c values of pure PA 12 could also be explained by a recrystallization processes during scanning in the calorimeter[6,7] as confirmed by the density value (Table I) which would correspond to a $w_c(\rho)$ of about 25%.

The presence of two endothermal peaks, of which the first one (T') is quite slightly expressed at 170°C in the slowly cooled samples B and E and in the ad-

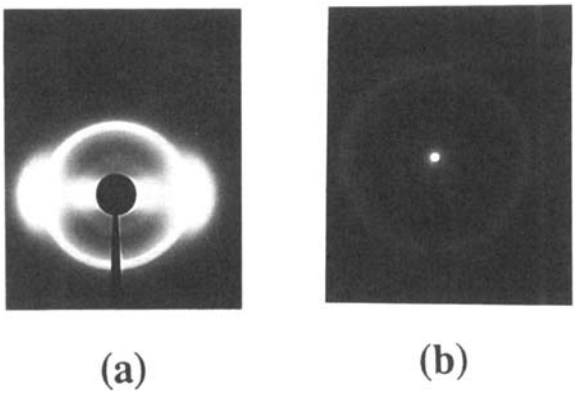

FIGURE 2 WAXS transmission photographs of CF-PA 12 laminate (a) and GF-PA 12 laminate (b).

ditionally isothermally annealed samples C and F (Table I), suggests the existence of a low number of small and imperfect crystallites in these laminates. They melt at about 170°C and some of them crystallize in a more perfect structure leading then to the main melting peak (T') at 180°C.

Table I shows also the degree of crystallinity (x_c) of the phase crystallized from the melt under isothermal (at 160°C) and non-isothermal conditions. The values are calculated from DSC exotherms of all samples. It is seen that the amount of crystallites resulting from the two different types of crystallization is practically the same in the respective CF and GF-containing samples; at the same time x_c is very close to the degree of crystallinity (w_c) of these samples. Furthermore, Table I shows that samples A, B and C have x_c and w_c values that are higher than those of samples D, E and F. It follows that the type of the reinforcing component plays an important role in the formation of the polymer matrix morphology in two respects: (a) as a nucleation agent affecting the crystallization kinetics, and (b) as a factor influencing the crystal structure at the fiber/matrix interface.

This is the case of the so-called transcrystallisation characterized by radial growth of crystallites around the fibers. These crystalline arrays differ in morphology from the spherulites arising in the bulk of the matrix.[8–11] It is known that such a columnar structure at the interface arises predominantly around carbon fibers while transcrystallization is very seldomly observed with glass fibers.[12,13] The difference originates from the different nature of both fiber types and hence their different nucleation ability.

Figure 4 shows curves of isothermal crystallization from the melt at 160°C of pure PA 12, CF- and GF-PA 12 laminates taken by DSC (Figure 4a) and hot-stage polarized light microscopy (Figure 4b). They are graphical presentations of the overall crystallization rate at constant temperature and can be divided into three parts, i.e. two horizontal straight lines of different level and an S-shaped part connecting them.

The time dependence of the primary crystallization can be described by Avrami equation: $æ = 1 - \exp(-Kt^n)$, where K is the rate constant, n is Avrami exponent and æ is the degree of crystallinity representing the ratio between the amount of

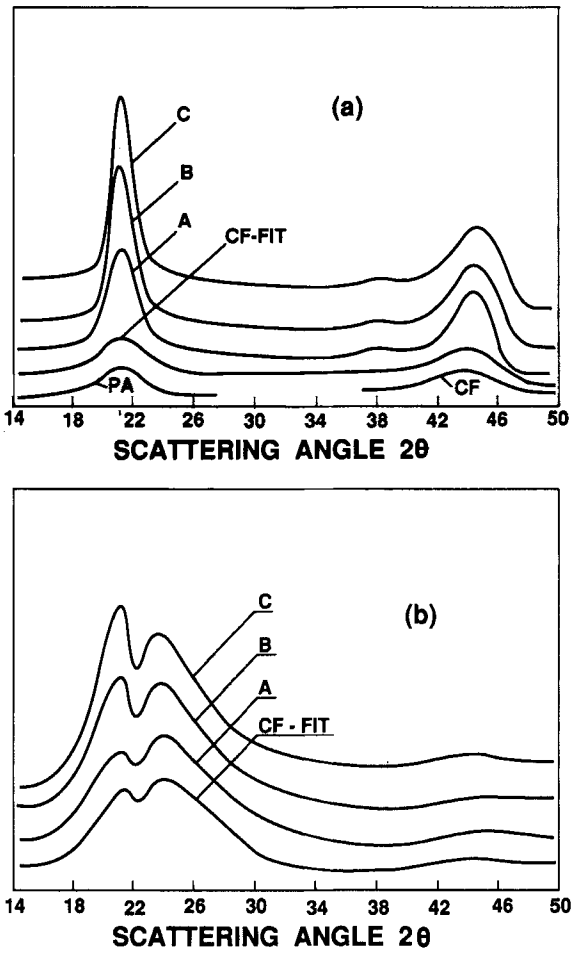

FIGURE 3 WAXS transmission diffractograms: (a) meridional and (b) equatorial scan of pure PA 12, CF-FIT, CF and CF-containing PA 12 laminate samples A, B and C.

the substance transformed into a crystalline phase at a certain time t and the total amount of the crystalline phase arising after completing of primary crystallization.

K and n were determined from the curves in Figure 4. Their numerical values for all samples are given in Table II. The K values decrease in the order CF-PA 12, pure PA 12, GF-PA 12 (Table IIa). This trend is observed also with pure PA 12 and PA 12 containing some carbon fibers only (Figure 4b, Table IIb). K was determined in this case from the isotherms taken by means of hot-stage polarized light microscopy.

It is well known that K is proportional to the nucleation ($\tilde{N}$) and crystal growth ($\tilde{A}$) rate, i.e. $K \sim \tilde{N}\tilde{A}$. Since K is determined by the temperature coefficients of $\tilde{N}$ and $\tilde{A}$ and the latter strongly depend on the supercooling (ΔT), it follows that the rate constant is a function of ΔT. Since in the case of isothermal crystallization ΔT is constant ($\Delta T = 60°C$) and the rate of crystal growth ($\tilde{A}$) under these conditions

TABLE I

Physical parameters of pure PA 12, CF-PA 12 and GF-PA 12 laminates

Sample		T′ [°C]	T″ [°C]	ρ [kg m^{-3}]	w_c(DSC) [%]	D [Å]	x_c (DSC) after Crystallization from the Melt [%]	
							non-isothermal	isothermal
Pure PA 12		-	178	1.022	42	37	28	26
CF-PA 12	A	-	178	1.415	44	36	40	39
	B	170	178	1.422	38	45	38	36
	C	173	181	1.426	40	45	41	38
GF-PA 12	D	-	179	1.752	37	70	33	31
	E	168	180	1.758	32	88	27	28
	F	171	180	1.761	34	95	29	27

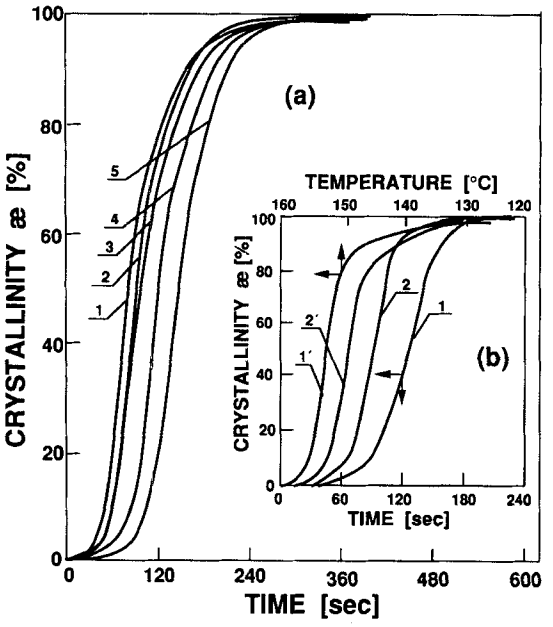

FIGURE 4 Crystallization isotherms taken by DSC (a): 1—CF-PA 12 laminate; 2—pure PA 12; 3—GF-PA 12 laminate; 4—CF-FIT; 5—GF-FIT; and by hot-stage polarized light microscopy (b): 1—pure PA 12; 2—PA 12 containing a small number of carbon fibers. 1′ and 2′-non-isothermal crystallization of the same samples.

is also constant, it can be assumed that K depends mainly on the nucleation rate ($\dot{N}$), i.e. $K \sim \dot{N}$ since the nucleation conditions differ from sample to sample. This assumption is confirmed by the values of the induction period (τ) and crystallization half time ($\tau_{1/2}$) of the materials studied. As seen in Table II, these values are much lower for the CF-PA 12 laminates which in turn is another proof of the nucleation ability of carbon fibers. The values of the Avrami exponent n in Table II are an indication for the three-dimensional growth of the crystallites in the samples.

TABLE II

Kinetic parameters of isothermal crystallization of PA 12 at 160°C determined by means of DSC and hot-stage polarizing microscopy

Sample	K	n	Crystallization Half Time $\tau_{1/2}$ [sec]	Induction Period τ [sec]
(a) Data from DSC				
Pure PA 12	1.0×10^{-6}	3.0	90	38
GF FIT	1.6×10^{-8}	3.5	138	56
CF FIT	3.6×10^{-8}	4.4	114	40
GF - PA 12 Laminate	3.1×10^{-7}	3.1	88	38
CF - PA 12 Laminate	2.6×10^{-6}	2.7	78	21
(b) Data from Microscopy				
Pure PA 12	1.4×10^{-9}	4.2	106	54
PA 12 with some CF	2.0×10^{-7}	3.3	90	37

Figure 4b shows the curves of isothermal and non-isothermal crystallization of pure PA 12 (Figure 4b, curves 1 and 1′) and PA 12 containing only some carbon fibers (Figure 4b, curves 2 and 2′) as taken by hot-stage polarized light microscopy. The steeper slopes of curves 1′ and 2′ suggest a higher crystallization rate in case of non-isothermal crystallization. However, calorimetric (Table I) and photographic (Figure 1) investigations show that the volume fraction and size of the crystallites in these samples are almost the same for both types of crystallization, i.e., the same morphological state of the matrix is attained regardless of the total crystallization rate. Nevertheless, it should be stressed that this assumption is valid solely at moderate cooling rates (in the present case 10°C/min). Higher cooling rates could result in the absence of nucleation and growth, i.e. $K \sim \tilde{N}\tilde{A} \sim 0$.

Actually this state was attempted to be achieved by means of the very rapid cooling (250°C/min) of some samples after consolidation in the mold (samples A and D, Table I). However, due to the chemical and physical nature of PA 12 (very flexible macromolecules and relatively low glass transition temperature), these attempts for reaching an amorphous polymer matrix proved to be unsuccessful. Under this cooling rate, a great number of relatively small and imperfect crystallites arose, and their volume fraction was higher in CF-PA 12 laminates due to the stronger nucleation effect of the carbon fibers.

As already mentioned, slower cooling favours both nucleation rate (mostly in CF-PA 12) and crystal growth which in turn leads to a larger size and/or a greater amount of crystallites and thus to a higher overall density of the composite (Table I, samples B and E). Additional isothermal treatment at 150°C does, however, not result in substantial changes in the polymer morphology, as seen in Table I (compare samples C and B, as well as E and F). The slight increase of the density is mainly due to a perfection of the crystallites. The somewhat increased crystallite size in sample F and the lack of crystallite growth in sample C (Table I) suggest that the very dense packing of reinforcing elements in the laminates hinders further crystal growth, especially in CF-PA 12 composites. Hence it can be concluded that on the one hand carbon fibers favour crystallization in laminates by their nucleation effect

and on the other hand they suppress crystal growth. Consequently, it can be assumed that almost the entire crystalline phase in these laminates is built up by transcrystalline layers around the carbon fibers. Such a structure has been also observed by other researchers.[14,15]

III.2. Mechanical Properties of Laminates

Some mechanical properties of CF- and GF-PA 12 laminates as calculated from the stress-strain curves of 3PB-tests are presented in Table III. The data are averaged from 5 measurements. The values of flexural strength (σ_{max}) and flexural modulus (E_{flex}) of the two rapidly cooled samples A and D are much lower than those of slowly cooled (B and E) and additionally annealed laminates (samples C and F). These differences are more substantial (almost double) in the case of CF-PA 12 laminates. The very close values of σ_{max}, E_{flex} and deflection at rupture (δ) in case of samples B and C, on the one hand, and for samples E and F on the other, can be attributed to the almost identical crystalline structure of these samples (Table I). In addition to the less perfect crystalline structure, the lower mechanical parameters of the rapidly cooled samples A and D are obviously due to macroscopic changes during their preparation, i.e. defects such as microcavities, disorientation of the fibers and poor consolidation between the bundles. They can be considered as a result of the absence of pressure during the cooling treatment which is clearly demonstrated by the greater thickness of these samples (by about 0.4–0.6 mm).

For the same reasons, it is very probable that the values of G_{Ic} and G_{IIc} of samples A are lower than those of samples B and C. It was established[1] that the G_{Ic} and G_{IIc} of the rapidly cooled GF-PA 12 laminates are two or three times higher than those of CF-PA 12 sample A (Table III).

Furthermore, an almost linear decrease of G_{Ic} and G_{IIc} with the rise of volume fraction and size of the crystallites was observed with GF-PA 12 laminates. As seen in Table III, the values of interlaminar fracture energies of CF-PA 12 laminates (samples B and C) are practically the same.

Figure 5 shows load-displacement plots obtained in mode I and mode II tests of CF-PA 12 laminates. After a typical elastic deformation of the samples, the energy stored so far is released by crack extension at a critical load. It should be noted,

TABLE III

Mechanical properties of CF-PA 12 and GF-PA 12 laminates

Sample		Strength [MPa]	E_{flex} [GPa]	Deflection [mm]	G_{Ic} [kJ/m²]	G_{IIc} [kJ/m²]	L/h
CF-PA 12	A	384	58	5,6	1.8	1.6	34
	B	720	104	4.6	2.4	1.9	34
	C	712	101	4,4	2.6	2.0	34
GF-PA 12	D	390	36	6.3	4.0*	4.1*	25
	E	572	40	5.7	3.3*	3.5*	25
	F	550	41	5.4	2.6*	3.1*	25

* Results from our previous study [Ref. 1]

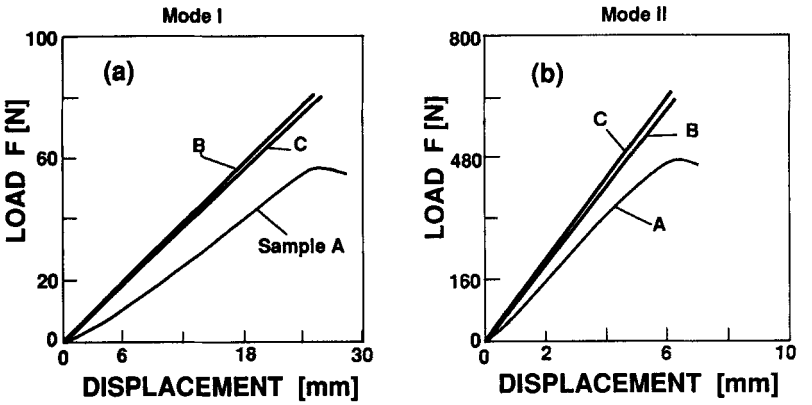

FIGURE 5 Load-displacement plots of various carbon-fiber reinforced polyamide 12 composite laminates tested under mode I (a) and mode II (b) conditions.

however, that a very short crack propagation (0.5–1 mm) was observed, followed by breakage of all samples.

As it is known, the interlaminar fracture mechanisms in thermoplastic matrix composites are associated with an extensive ductile matrix deformation which occurs in a damage zone ahead of the crack tip, especially when spreading over several fiber diameters. This leads to a great amount of fiber bridging within the main crack and to the build-up of side cracks.[16] In case that the fiber-matrix bonding is poor, the crack runs along the fiber interfaces and only in-between the fibers the matrix fails in a ductile manner. However, when a mostly transcrystalline structure is generated around densely packed reinforcing elements and when the bonds are rather strong as in the case of carbon fibers, a brittle fracture of the matrix may take place. This is the basic reason for the brittle properties of CF-PA 12 laminates as a whole and hence for the lower values of G_{Ic} and G_{IIc} of the samples as compared to those of GF-containing laminates (Table III).

IV. CONCLUSION

In order to describe the morphological changes occurring during the processing of polyamide 12 composites, the crystallization kinetics, the volume fraction and the size of the crystallites as a function of the type of the reinforcing component and the thermal pre-history have been analyzed. It could be established that due to the nucleation ability of carbon fibers CF-PA 12 laminates show a faster crystallization rate and a relatively higher degree of crystallinity than GF-PA 12 composites. Carbon fibers affect the crystal structure at the fiber/matrix interface, generating mostly transcrystalline layers around the fibers. Such a columnar structure around densely packed reinforcing components improves the fiber/matrix adhesion and is also strongly reflected in the properties of the laminates. CF-PA 12 laminates have been found to possess high values of flexural strength and modulus but lower G_{Ic}- and G_{IIc}-values when compared to GF-PA 12 composites.

Acknowledgment

The authors gratefully acknowledge the financial support of the German Department of Research and Technology, in particular under project BMFT 227-9211-BUL, No. 218.2 and of the Bulgarian Ministry for Education and Science. Further thanks are due to the Fonds der Chemichen Industrie, Frankfurt, for Prof. Friedrich's personal research activities in 1991.

References

1. H. Wittich, M. Evstatiev, E. Bozwelieva, K. Friedrich and S. Fakirov, Adv. Composite Materials, Japan, (1991), in press.
2. Atochem Reports, Thermoplastic Polymer in Powders for Composites, Atochem, Paris, 1985.
3. J. E. Stamhuis and A. J. Pennings, *Polymer*, **18**, 67 (1977).
4. B. D. Cullity, in "Elements of X-Ray Diffraction," Addison-Wesley Publ., Reading, Massachusetts, 1978.
5. L. Carlsson and R. B. Pipes, "Experimental Characterization of Advanced Composite Materials" (Eds.), Prentice Hall Inc., 1987.
6. S. Fakirov, E. W. Fischer, R. Hoffman and G. F. Schmidt, *Polymer*, **18**, 1121 (1977).
7. S. Fakirov, *Vyssokomol. soed. (A)* **32**, 878 (1990) (in Russian).
8. C. M. Tung and P. J. Dynes, *J. Appl. Polym. Sci.*, **33**, 505 (1987).
9. R. H. Burton, T. M. Day and M. J. Folkes, *Polym. Communications*, **25**, 361 (1984).
10. B. Chaberst, J. Chauchard and J. Cinquin, *Mak. Chem. Macr. Symp.*, **9**, 99 (1987).
11. L. Caramaro, B. Chabert and J. Chauchard, *C. R. Acad. Sci. Paris*, **306**, 887 (1988).
12. T. Bessel and J. B. Shortall, *J. Matter Sci. Letters*, **3**, 1071 (1984).
13. R. H. Burton and J. M. Folkes, *Plastics and Rubber Processing and Applications*, **3**, 129 (1983).
14. T. Bessel, D. Huii and J. B. Schortall, *Faraday Spec. Discus. Chem. Soc.*, **2**, 137 (1972).
15. S. Saiello, J. Kenny and L. Nicolais, *J. Mater. Sci.*, **25**, 3493 (1990).
16. K. Friedrich, (Ed.), "Application of Fracture Mechanics to Composite Materials," Elsevier Sci. Publ., Amsterdam, 1989.